ECSE-525 Satellite Navigation Systems
Fall 2025

Ali Seifeldin

Final Project Report:
LEO Constellation Simulation and Ground Station Visibility Analysis

Abstract

Low Earth Orbit (LEO) satellite constellations have emerged as a critical component of modern space-based communication, navigation, and Earth observation systems. Their low altitude enables reduced latency, improved geometric diversity, and fast-changing visibility patterns, making them highly relevant to next-generation Positioning, Navigation, and Timing (PNT) architectures.

This project simulates a LEO constellation and evaluates its visibility from a fixed ground station. Leveraging gnss_lib_py, the simulation computes satellite trajectories, elevation profiles, and PDOP / HDOP over a full orbital cycle. Results demonstrate that LEO satellites produce frequent visibility windows, yielding high revisit rates and dynamic spatial coverage. These characteristics highlight the potential benefits of LEO augmentation for continuous connectivity and enhanced navigation geometry.

1. Introduction

Low Earth Orbit (LEO) satellite constellations have rapidly expanded in scale and capability over the past decade. Originally deployed to deliver global broadband connectivity, these constellations have also demonstrated significant potential to support next-generation Positioning, Navigation, and Timing (PNT) services. Their low orbital altitude, typically between 160 and 2000 km, offers several inherent advantages over traditional Medium Earth Orbit (MEO) Global Navigation Satellite Systems (GNSS), including reduced communication latency, substantially stronger signal power, and faster-changing satellite–receiver geometry. These characteristics motivate growing interest in exploring how LEO systems can augment or complement existing GNSS infrastructure.

At the same time, classical GNSS faces well-known limitations. Signals arriving from MEO satellites are weak after traveling nearly 20,000 km, making them vulnerable to blockage, multipath, and interference—particularly in dense urban environments or indoor settings. Positioning accuracy also depends heavily on satellite geometry; when satellites cluster over similar directions in the sky, Dilution of Precision (DOP) increases, reducing the robustness of the solution. LEO satellites, by virtue of their altitude and orbital motion, naturally provide stronger signals and richer geometric diversity, offering an opportunity to enhance positioning performance, improve integrity, and increase availability in challenging environments.

Motivated by these emerging capabilities, this project investigates the geometric and visibility characteristics of LEO constellations from a ground-based receiver perspective. Using precise GNSS orbit data (SP3), propagated LEO ephemerides, and elevation-based visibility filtering, the simulation evaluates satellite visibility, and Position Dilution of Precision (PDOP) over time. By comparing GNSS-only configurations with hybrid GNSS+LEO scenarios, the study provides insight into how the inclusion of LEO satellites improves satellite availability and strengthens positioning geometry.

The goal of this work is not to perform full PNT estimation, but rather to quantify the geometric benefits that LEO satellites introduce when integrated into a conventional GNSS framework. The resulting analysis highlights the rapid revisit rates, enhanced visibility, and improved PDOP enabled by LEO systems, findings that reinforce the growing consensus that LEO constellations will play a key role in future hybrid navigation architectures.

2. Literature Review

Low Earth Orbit satellite constellations, including prominent examples like SpaceX Starlink, OneWeb, and Amazon Kuiper, are rapidly advancing space-based services by deploying numerous low-altitude satellites to offer global broadband and positioning capabilities. Existing literature consistently highlights the inherent advantages of LEO architectures over traditional GNSS Medium Earth Orbit systems. These benefits encompass lower communication latency, expanded global reach, and a dense geometric distribution of satellites (Oak et al., 2023). Furthermore, the rapid movement of LEO satellites relative to Earth provides high temporal diversity, which is crucial for dynamic PNT applications.

The lower orbital altitude of LEO satellites results in significantly stronger signals, often reported as 25-30 dB more potent than GNSS signals (Shi et al., 2023; Yang et al., 2025). LEO satellites are approximately 20 times closer to Earth than MEO satellites, resulting in signal strengths 300 to 2400 times more powerful than GNSS (El-Mowafy et al., 2023). This enhanced signal strength improves signal penetration and anti-interference capabilities, enabling more robust PNT in challenging environments.

Studies have extensively validated the use of LEO satellites to substantially enhance GNSS positioning capabilities. Due to their proximity to Earth, LEO satellites provide superior geometry for Dilution of Precision metrics. Research indicates that LEO augmentation can dramatically reduce PDOP values, with simulated improvements showing significant percentage decreases. Specifically, the geometric configuration offered by LEO constellations can be up to three times better than that of current GNSS constellations, leading to a notable improvement in positioning accuracy (Hein, 2020). Optimized LEO constellation designs have been shown to reduce the Geometry Dilution of Precision for global ground users to below 5 (Yang et al., 2024), thereby improving the accuracy, integrity, and availability of PNT services.

The effectiveness of LEO augmentation on GNSS performance is directly related to the number and geometric distribution of satellites within the constellation (Hong et al., 2023). The integration of LEO systems provides a robust backup and supplementation for GNSS, particularly in environments where GNSS signals may be unreliable or unavailable, such as urban canyons or areas susceptible to jamming (Guo et al., 2023; Singh et al., 2022). In these challenging environments, the increased number of ranging measurements from mega-constellations significantly enhances robustness by optimizing observation geometry and increasing the number of visible satellites (García-Fernández, 2024; Racelis et al., 2019).

Recent research has further demonstrated the benefits of integrating LEO satellites with GNSS, particularly in challenging or signal-degraded environments (Çelikbilek et al. 2024). A detailed performance assessment combining existing GNSS constellations with prospective LEO-PNT

systems under indoor non-line-of-sight conditions was conducted, showing that the inclusion of LEO satellites can raise signal coverage to nearly 100%, compared with the significantly lower availability of standalone GNSS. Their simulations also indicate that LEO augmentation can lower path-loss by approximately 25 dB and improve DOP metrics by around 45% on average, highlighting the contribution of LEO geometry and link-budget advantages to positioning reliability. Importantly, the study also notes that constellation combinations must be selected carefully, as adding more systems does not always yield better geometry or carrier-to-noise ratios. These findings reinforce the central premise of this project: that LEO constellations, when properly integrated with GNSS, can substantially enhance PNT performance in environments where traditional GNSS is insufficient.

3. Background Theory

3.1 Coordinate Systems and ECEF Conversion

Satellite and receiver coordinates in this work are expressed in the Earth-Centered Earth-Fixed (ECEF) frame, which rotates with the Earth and provides a stable reference for ground-based users. The receiver position is initially defined in geodetic latitude, longitude, and height on the WGS-84 ellipsoid, and then converted into ECEF using the standard ellipsoidal transformation:

$$N(\phi) = \frac{a}{\sqrt{1 - e^2 sin^2 \phi}},$$

$$x = (N(\phi) + h)\cos\phi\cos\lambda,$$

$$y = (N(\phi) + h)\cos\phi\sin\lambda$$

$$z = (N(\phi)(1 - e^2) + h)\sin\ \phi$$

Here, a is the semi-major axis and e is the eccentricity of the WGS-84 ellipsoid. Satellite positions from precise SP3 files are already provided in ECEF. Establishing all satellite and receiver coordinates in a common ECEF frame enables consistent computation of line-of-sight vectors and geometric relationships used throughout the simulation.

3.2 Satellite–Receiver Geometry, Elevation Angle, and Visibility

Once positions are available in ECEF, the line-of-sight (LOS) vector between the receiver and a satellite is computed as:

$$\boldsymbol{\rho}_i = \mathbf{r}_{\mathrm{sat},i} - \mathbf{r}_{\mathrm{rx}},$$

where $\mathbf{r}_{\text{sat},i}$ is the ECEF position of satellite i and $\mathbf{r}_{\text{rx}}$ is the receiver's ECEF position. To determine visibility, the LOS vector is transformed into the local topocentric East-North-Up (ENU) frame, from which elevation and azimuth are obtained:

$$\text{el}_i = \arctan\ 2(\rho_U, \sqrt{\rho_E^2 + \rho_N^2}),$$
$$\text{az}_i = \arctan\ 2(\rho_E, \rho_N).$$

A satellite is considered visible only when its elevation angle exceeds a chosen elevation mask. In our experiment, we vary this from $10°$–$60°$ to simulate different environments. This filtering realistically models signal blockage and attenuation near the horizon and is essential for comparing GNSS-only and GNSS+LEO constellations under consistent visibility assumptions.

3.3 Dilution of Precision (DOP) and Geometric Observability

To compute Dilution of Precision, the satellite geometry is encoded in the design matrix $\mathbf{H}$, which is built directly from the line-of-sight (LOS) vectors between the receiver and all visible satellites. For each satellite i, the ECEF line-of-sight vector is computed as $\boldsymbol{\rho}_i = \mathbf{r}_{\text{sat},i} - \mathbf{r}_{\text{rx}}$, and the corresponding LOS unit vector is

$$\mathbf{e}_i = \frac{\boldsymbol{\rho}_i}{\| \boldsymbol{\rho}_i \|} = \begin{bmatrix} e_{ix} \\ e_{iy} \\ e_{iz} \end{bmatrix}.$$

The row of the geometry matrix associated with satellite i consists of the negative LOS components and a final column representing the receiver clock bias:

$$\mathbf{h}_i = [-e_{ix} \quad -e_{iy} \quad -e_{iz} \quad 1].$$

Stacking these rows for all n visible satellites yields the full geometry matrix

$$\mathbf{H} = \begin{bmatrix} \mathbf{h}_1 \\ \mathbf{h}_2 \\ \vdots \\ \mathbf{h}_n \end{bmatrix}.$$

Positioning accuracy depends strongly on the spatial geometry of visible satellites. This geometry is captured through the linearized pseudorange observation model:

$$\Delta\boldsymbol{\rho} = \mathbf{H}\,\Delta\mathbf{x} + \boldsymbol{\varepsilon},$$

where $\Delta\mathbf{x} = \Delta\mathrm{x}, \Delta\mathrm{y}, \Delta\mathrm{z}, \Delta t]^T$ contains receiver position and clock corrections, and $\mathbf{H}$ is the geometry (design) matrix built from LOS unit vectors and a clock term. Assuming equal measurement noise variance σ^2, the covariance of the estimated state is:

$$\mathbf{Q} = \sigma^2(\mathbf{H}^\mathrm{T}\mathbf{H})^{-1}.$$

Dilution of Precision (DOP) metrics are extracted from the diagonal elements of $\mathbf{Q}$. The main quantities used in this work are:

$$\mathrm{PDOP} = \sqrt{\sigma_x^2 + \sigma_y^2 + \sigma_z^2},$$

$$\mathrm{HDOP} = \sqrt{\sigma_x^2 + \sigma_y^2}$$

Different DOP values are computed from the diagonal terms of Q, each representing how geometry affects a specific component of the solution – we will focus on PDOP, which uses the variances in X, Y, and Z in the Q matrix. It represents the expected error amplification in 3D position and directly reflects how well the satellites "surround" the receiver in three-dimensional space. This paper will focus on PDOP, as well as HDOP, which is a PDOP with a fixed/known height. PDOP calculations require at least 4 satellites, while HDOP requires 3.

A lower DOP values indicate better geometry and more accurate positioning:

< 1: Excellent (ideal geometry)

1–2: Very good

2–5: Good (typical open sky)

5–10: Moderate (reduced accuracy)

>10: Poor geometry; unreliable solution

Because LEO satellites orbit at much lower altitudes and move quickly across the sky, they often provide favorable geometric diversity, especially in regions where GNSS satellites are blocked by buildings or terrain. As a result, adding LEO satellites to a GNSS-only solution can significantly reduce PDOP, improve vertical geometry, and increase overall satellite availability.

4. Simulation Methodology

4.1 Tools and Environment

The simulation is implemented in Python using a combination of scientific computing libraries and GNSS-specific toolkits. The primary dependency is gnss_lib_py (Knowles et al., 2024), an open-source library designed for GNSS data processing, coordinate conversions, and Dilution of Precision (DOP) computation. This library provides built-in tools for transforming between coordinate reference frames, computing line-of-sight geometry, and evaluating PDOP/HDOP metrics using standard formulations from satellite navigation theory.

To simulate GNSS satellite positions, the experiment uses a SP3 format: COD0MGXFIN_20211180000_01D_05M_ORB.SP3, which contains high-accuracy orbital positions for GPS, GLONASS, BeiDou, and other GNSS satellites at 5-minute intervals for April 28, 2021. SP3 files offer centimeter- to decimeter-level accuracy and are suitable for geometry-based performance analysis and is provided in the gnss_lib_py library.

To model LEO satellites, orbital data for the Starlink network is extracted from the Space-Track API (Space-Track). Approximately 1000 “good” satellites are selected, where “good” is defined as operational, non-decayed Starlink spacecraft with orbital altitudes between 600 km and 2000 km. These data originate from Two-Line Element (TLE) sets, which are propagated forward to produce Earth-Centered Inertial (ECI) positions. The resulting trajectories are interpolated to 5-minute intervals and time-aligned with the GNSS SP3 timestamps. This alignment is required because GNSS and TLE data sources do not share identical epochs. Although the exact historical Starlink constellation matching the SP3 epoch is unavailable, this assumption enables a consistent comparison of GNSS-only and GNSS+LEO geometries.

4.2 Simulation Parameters and Workflow

The simulation follows a structured workflow designed to evaluate satellite visibility and geometric performance from a fixed ground station.

- Step 1: Define Ground Receiver Position
    - A single receiver is placed at a fixed geodetic location (latitude, longitude, height).
    - This location is transformed into the ECEF coordinate frame using the standard WGS-84 ellipsoidal conversion equations – we selected Montreal as the base for this experiment.
- Step 2: Load and Preprocess Satellite Orbits
    - GNSS satellite positions are extracted from the SP3 file and converted to ECEF (already provided in SP3).

    - Starlink LEO satellites are propagated from TLEs, converted from ECI to ECEF, and indexed by matching timestamps.
- Step 3: Satellite–Receiver Geometry
    - For each timestamp:
    - Compute the line-of-sight vector and compute elevation and azimuth angles.
    - Apply an elevation mask between 10° and 60°, representing different environmental obstructions. Only satellites above the mask are considered visible.
- Step 4: Compute DOP Values
        - PDOP values are computed using gnss_lib_py
- Step 5: Compare GNSS-Only vs GNSS+LEO
    - For each epoch and for each elevation mask:
    - Count satellites in view
    - Compute DOP metrics
    - Visualize time-varying performance

This enables quantitative comparison of how LEO satellites enhance geometry and visibility compared to GNSS-alone baselines.

4.3 Key Assumptions and Limitations

Several simplifying assumptions are made to focus the analysis on geometric performance rather than full navigation accuracy:

- TLEs provide approximate orbit predictions and are not as precise as SP3 data. However, for DOP studies, geometric relationships matter more than sub-meter accuracy.
- LEO and GNSS data are aligned by interpolation rather than using their original epoch spacing. This ensures consistent geometric evaluation but assumes quasi-stationary behavior across short intervals.
- No measurement noise modeling, DOP predicts error amplification but not absolute error—ideal for geometry studies.

These assumptions are appropriate for evaluating the feasibility and potential benefit of LEO-assisted GNSS from a geometric standpoint.

5. Results & Discussion

The GNSS data was imported from the SP3 file and GP01, GP03 and GP04 of the GPS constellation were plotted along their ECEF X axis. This is a sanity check to show that the satellites positions were correctly imported as seen in Figure 1.

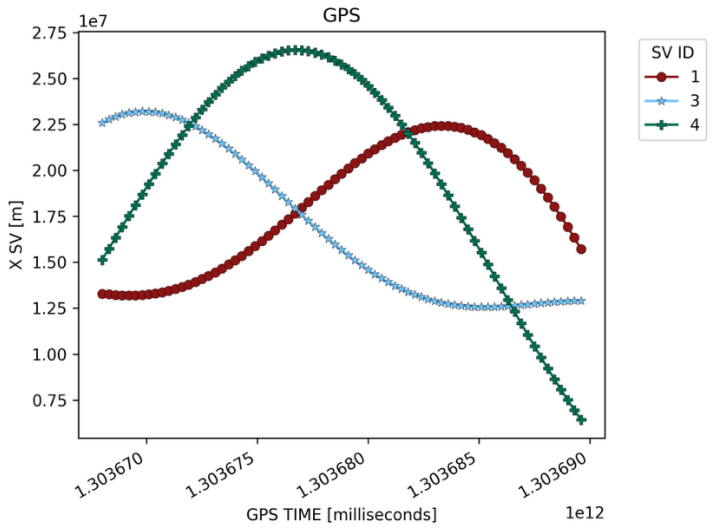

Figure 1

5.1 GPS analysis

The analysis begins with a pure GPS constellation. A base station is placed in Montreal at coordinates 45.5017, -73.5673 with an elevation of 30 meters. For each timestep, the number of visible satellites from the base station is computed using an elevation mask. If a satellite's elevation angle is below this mask, it is considered not visible, as illustrated in Figure 2.

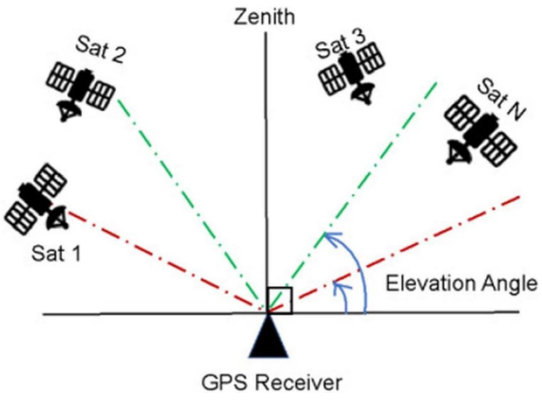

Figure 2

Figure 3 presents the number of visible satellites for several elevation mask values. Simulations are performed for masks of 10, 15, 20, 30, 40, 50, and 60 degrees. A mask of 10 to 15 degrees represents an open field, 30 degrees corresponds to environments with moderate obstructions, and 60 degrees reflects conditions similar to an urban canyon. As expected, the number of visible satellites decreases as the elevation mask increases.

This reduction is significant because at least four satellites are required to compute PDOP, and a minimum of three is needed for HDOP when the height is known. Once the mask reaches 40 degrees and higher, the number of visible satellites regularly drops to around four or fewer. In

these cases, PDOP becomes unstable, often exceeding 10 for a mask of 40 degrees and occasionally even for a 30-degree mask, indicating poor satellite geometry. HDOP performs somewhat better but still produces values above 10 when the mask is 50 degrees or more. Ideally, PDOP values should be close to 1 and should not exceed 5.

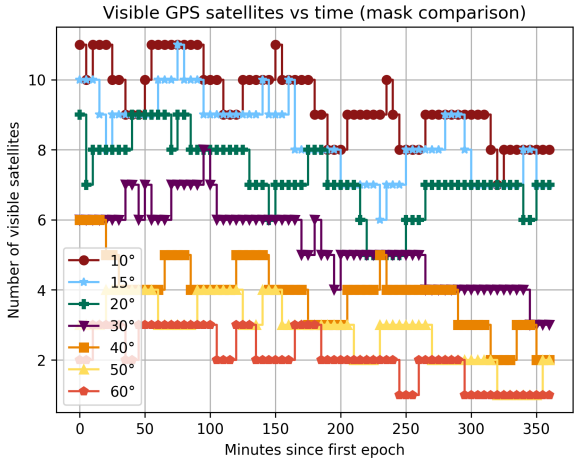

Figure 3

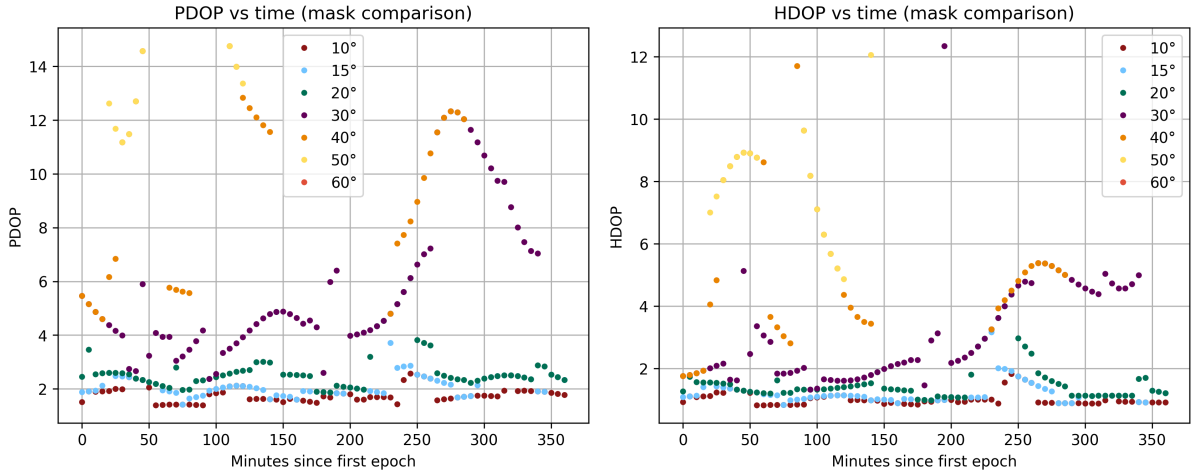

Figure 4

5.2 GPS + LEO augmentation analysis

After completing the analysis on a pure GPS constellation, we extend the simulation to include an additional LEO constellation composed of 1000 Starlink satellites. The goal is to examine how augmenting GPS with a dense LEO layer affects satellite visibility and the resulting dilution of precision values under the same elevation mask conditions. The same base station in Montreal is used, and the elevation masks of 10, 15, 20, 30, 40, 50, and 60 degrees are again applied for consistency.

Introducing a LEO constellation greatly increases the number of visible satellites across all elevation masks, as shown in Figure 5. Even at high mask values such as 50 or 60 degrees, the combined GPS+LEO system maintains a large set of visible satellites at nearly every timestep. This contrasts with the GPS-only case, where visibility often drops close to or below the minimum needed for stable DOP estimation once the mask exceeds 40 degrees.

This increased visibility leads to stronger positioning geometry. HDOP stays low for all elevation masks, with only rare spikes, and even at 60 degrees it remains well within acceptable levels throughout most of the simulation. PDOP shows a similar improvement. The high and unstable PDOP values observed in the GPS-only results for 30- and 40-degree masks no longer appear when LEO satellites are included. At a 50-degree mask, PDOP generally remains between 4 and 9, indicating that although accuracy decreases somewhat, the system is still able to maintain a usable position solution.

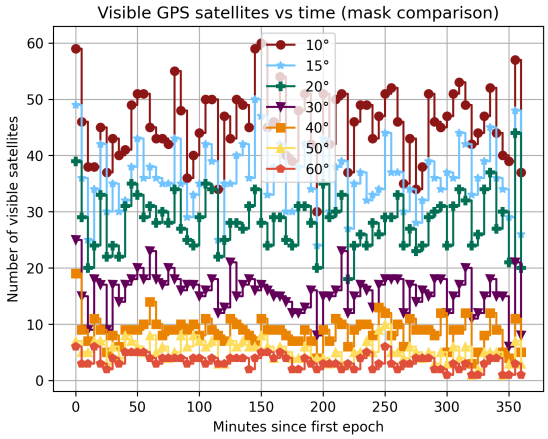

Figure 5 – 1000 LEO satellites

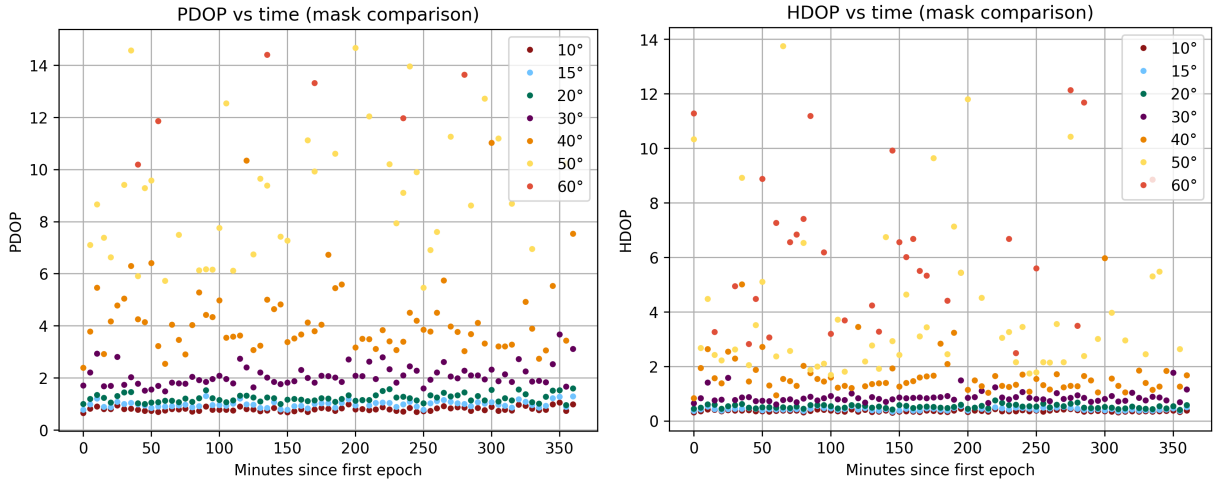

Figure 6 – 1000 LEO satellites

Overall, integrating LEO satellites with GPS greatly enhances both the availability and the quality of positioning geometry. The dense LEO layer compensates for satellite losses caused by high elevation masks, allowing the system to maintain strong visibility and more stable DOP values even under urban-canyon-like conditions.

5.3 Additional analysis and results

Additional analysis was conducted to evaluate the impact of increasing the LEO constellation size and to compare alternative GNSS constellations. Expanding the LEO constellation from 1000 to 3000 satellites resulted in a higher number of visible satellites across all elevation masks, with some slight improvements in PDOP as seen in Figure 7.

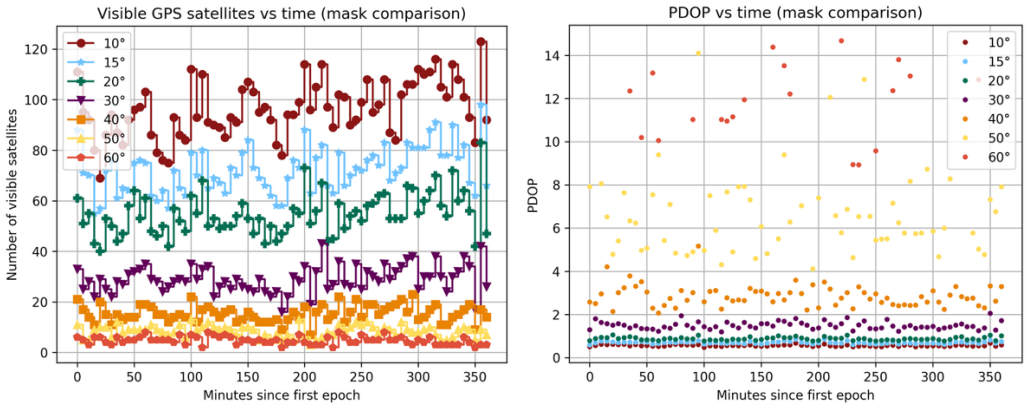

Figure 7 - 3000 LEO satellites

A parallel analysis using BeiDou or GLONASS in place of GPS produced results consistent with the GPS+LEO case. The overall visibility patterns and DOP behavior were nearly identical, showing that the addition of a dense LEO constellation dominates the geometry and reduces dependence on which specific GNSS constellation is used.

Conclusion

This project examined the performance of the GPS and GPS+LEO satellite constellations from a receiver located in Montreal, focusing on satellite visibility and geometric dilution of precision (PDOP and HDOP). Using python simulations and published orbital parameters for both systems, we evaluated how each constellation's geometry changes throughout the day and how these variations affect positioning accuracy.

When both constellations are used together, the combined system demonstrates significantly improved performance. Increased satellite availability reduces geometric dilution at all times of the day, leading to more stable and accurate positioning. This reinforces the advantage of GNSS augmentation with LEO, which can exploit complementary geometries to ensure robust navigation even when one system temporarily experiences weaker geometry.

References

1. Alghisi M, Zallemi N, Biagi L. Improvements in PPP by Integrating GNSS with LEO Satellites: A Geometric Simulation. Sensors. 2025; 25(14):4427. https://doi.org/10.3390/s25144427

2. Oak, Sukrut, Pullen, Sam, Lo, Sherman, Colobong, Isaiah, Blanch, Juan, Walter, Todd, Crews, Mark, Jackson, Robert, "GNSS Augmentation by Low-Earth-Orbit (LEO) Satellites: Integrity Performance Under Non-Ideal Conditions," Proceedings of the 36th International Technical Meeting of the Satellite Division of The Institute of Navigation (ION GNSS+ 2023), Denver, Colorado, September 2023, pp. 1436-1453. https://doi.org/10.33012/2023.19455

3. W. Li, Q. Yang, X. Du, M. Li, Q. Zhao, L. Yang, Y. Qin, C. Chang, Y. Wang and G. Qin, "LEO augmented precise point positioning using real observations from two CENTISPACE™ experimental satellites," GPS Solutions, vol. 28, no. 1, Art. no. 44, 2024. http://doi.org/10.1007/s10291-023-01589-0

4. C. Shi, Q. Guo, Z. Li, G. Jing and Y. Zhang, "RTK from space: a novel and low-cost GNSS augmentation technique for LEO communication satellites," GPS Solutions, vol. 29, Art. no. 80, 2025. http://doi.org/10.1007/s10291-025-01837-5

5. El-Mowafy, A.; Wang, K.; Li, Y.; Allahvirdi-Zadeh, A., "The Impact of Orbital and Clock Errors on Positioning from LEO Constellations and Proposed Orbital Solutions," Int. Arch. Photogramm. Remote Sens. Spatial Inf. Sci., vol. XLVIII-1/W2, pp. 1111-1117, 2023. https://doi.org/10.5194/isprs-archives-XLVIII-1-W2-2023-1111-2023

6. G. W. Hein, "Status, perspectives and trends of satellite navigation," Satellite Navigation, vol. 1, no. 1, Article 3, 2020. https://doi.org/10.1186/s43020-020-00023-x

7. Y. Yang et al., “Demand and key technology for a LEO constellation as navigation augmentation,” Satellite Navigation, vol. 5, Article 33, 2024. https://doi.org/10.1186/s43020-024-00133-w

8. Haibo Ge, Guanlong Meng, Bofeng Li, LEO enhanced GNSS (LeGNSS) precise point positioning with emphasis on model comparison, Advances in Space Research, Volume 74, Issue 5, 2024, Pages 2156-2168, ISSN 0273-1177, https://doi.org/10.1016/j.asr.2024.06.006

9. M. García-Fernández, “Mapping TLE orbital parameters to GNSS ephemeris for LEO-PNT mega-constellation orbit simulations and visibility analysis,” arXiv, Jan. 31, 2024, https://doi.org/10.48550/arXiv.2401.17767

10. D. Racelis, B. Pervan and M. Joerger, “Fault-Free Integrity Analysis of Mega-Constellation-Augmented GNSS,” in Proc. ION GNSS+, 2019, https://doi.org/10.33012/2019.16862

11. K. Çelikbilek and E. S. Lohan, "A Performance Study on the Combination of Available GNSS and Potential LEO-PNT Constellations," in IEEE Access, vol. 12, pp. 162909-162917, 2024, https://doi.org/10.1109/ACCESS.2024.3490892

12. Shi, C., Guo, Q., Li, Z. et al. RTK from space: a novel and low-cost GNSS augmentation technique for LEO communication satellites. GPS Solut 29, 80 (2025). https://doi.org/10.1007/s10291-025-01837-5

13. D. Knowles, A. V. Kanhere, D. Neamati, and G. Gao, “gnss_lib_py: Analyzing GNSS data with Python,” SoftwareX, vol. 27, 2024, Art. no. 101811. https://doi.org/10.1016/j.softx.2024.101811

14. E. Lodetti and A. Iseni, “SimuLEO: Low Earth Orbit Satellites Simulator,” GitHub repository. Available: https://github.com/emmalod/SimuLEO

15. “Space-Track,” Space Surveillance Network, SAIC, [online]. Available: https://www.space-track.org/ . [Accessed: 25-Nov-2025].